energy&fuels

Article

pubs.acs.org/EF

Oxidation Kinetics of Oil Shale Semicokes: Reactivity as a Function of Pyrolysis Temperature and Shale Origin

Jillian L. Goldfarb,*[,†] Anthony D'Amico,[†] Christopher Culin,[‡] Eric M. Suuberg,[‡] and Indrek Külaots[‡]

[†]Department of Chemical Engineering, University of New Hampshire, 33 Academic Way, Durham, New Hampshire 03824, United States

[‡]School of Engineering, Brown University, 182 Hope Street, Providence, Rhode Island 02912, United States

ABSTRACT: As an alternative fossil fuel garnering attention in the wake of unstable crude oil prices, oil shale faces several obstacles before its seemingly imminent commercialization. One of the largest environmental stumbling blocks to its widespread use is the primary byproduct of oil extraction processes: semicoke. With the majority of semicoke disposed of in open landfills, this waste stream poses a threat to the environment, and its disposal may well represent a waste of a potentially useable byproduct. Previous studies show that oil shale from Estonia, China, and the United States, pyrolyzed at 500 and 1000 °C at a rate of 20 °C min^{-1}, yield semicokes with relatively high organic char contents and high surface areas. To determine how shale origin and pyrolysis temperature impact the activation energy of oil shale semicoke combustion, we investigate the oxidation kinetics of oil shale semicokes pyrolyzed at these two temperatures. Activation energies in air are in the range of 108−130 kJ mol^{-1} for the semicokes pyrolyzed at 500 °C and 147−195 kJ mol^{-1} for samples pyrolyzed at 1000 °C. Depending on the oil shale pyrolysis temperature and extent of reaction, the semicoke oxidative reaction orders range from 0.55 to 0.72.

INTRODUCTION

Whether viewed as a long-term solution to dwindling conventional fossil fuel sources or as a bridge between pipelines in the Middle East and a renewable energy future, unconventional or alternative fossil fuels are of keen interest to public and private enterprises alike. The United States has vast deposits of oil shale,[1] which is a fine-grained sedimentary rock containing a proportionally large amount of kerogen, the organic portion in the shale rock that can be converted to oil by thermal degradation. The primary byproduct of current oil shale oil extraction processes is semicoke, which is a semicarbonaceous system that both poses a potential threat to groundwater via leaching of polycyclic aromatic hydrocarbons, heavy metals, and phenols that are entrained in the semicoke by rain and snow, and a logistical and physical threat to surrounding areas by the veritable mountains of semicoke produced.[2−6] The Estonian landscape is piled high with ∼300 million tons of ash and 110 million tons of semicoke.[7,8] Although some semicoke finds its way into construction materials such as concrete, rock wool, asphalts, bricks, and other uses, this represents a small fraction of the total semicoke produced,[9−11] One of the more efficient uses for oil shale semicoke is to be put back into the retorting process as a fuel burned for heating the raw shale, especially considering the energy-intensive nature of the retorting process,[4,12,13] or to further extract useable oil when combined with fresh shale.[14]

In Estonia, where a substantial majority of the country's electricity is generated from oil shale, both the Kiviter-type internal combustion vertical retorts and solid heat carrier units are used. In the former, some generator gas produced is used in oil shale retorting, while the rest is used in power plant boilers; however, in the latter system, semicoke is burned to obtain the solid heat carrier (ash) for the retorting, such that all the generator gas is used as fuel in the power plant boilers.[15] Semicoke, or organic char, has been shown to contain various amounts of organic carbon, ranging from 1.7 wt % to 17.5 wt %, with carbon content decreasing as the pyrolysis temperature increases.[16] [Note that "semicoke" is not referred to as organic carbon as it is a heterogeneous carbonaceous system of carbon and hydrogen with lesser amounts of sulfur, nitrogen and oxygen present.] However, its relatively low critical temperatures suggest an underlying strong reactivity. A limited amount of the oil shale literature probes the characteristics of oil shale semicokes;[17] the majority of the literature focuses on the oil shale retorting process, quantifying extractable oil, and general characteristics of the oil derived from shale. Here, we investigate the potential conversion of oil shale semicoke from a waste to a useable byproduct fuel by characterizing semicoke reactivity in oxygen to determine activation energies and reaction orders as a function of pyrolysis temperature and shale origin.

EXPERIMENTAL METHODS

A total of five oil shale samples, two originating from the Maoming mine (Guangdong Province, Southwest China, local classifications of A and C), one from the Aidu mine (northeast Estonia) and two from the Green River Formation (Colorado, USA, 19 and 50 GPT) were ground and sieved to yield samples of particle size between 45 μm and 75 μm. Approximately 5 g of each shale sample were placed in a porcelain boat and pyrolyzed in a laboratory tube furnace at one of two temperatures—500 and 1000 °C—at a rate of 20 °C min^{-1} under a helium flow of 300 cm^3 min^{-1} and held for 1 h at the final temperature. The 500 °C pyrolysis temperature represents an industrially applicable surface retort temperature. We pyrolyzed the second sample at 1000 °C (although this is certainly past the 650−700 °C upper bound for

Received: September 13, 2012
Revised: December 6, 2012
Published: December 11, 2012

Table 1. Isothermal Kinetic Parameters Used for Determination of Oxidation Activation Energies and Pre-exponential Factors for Oil Shale Semicokes

temperature (°C)	k (s^{-1})	temperature (°C)	k (s^{-1})	Temperature (°C)	k (s^{-1})
Colorado 19GPT 500 °C Pyrolysis		**Estonian 500 °C Pyrolysis**		**Chinese M-A 1000 °C Pyrolysis**	
352	1.01×10^{-4}	343	9.92×10^{-3}	460	1.60×10^{-2}
362	1.23×10^{-4}	348	1.18×10^{-2}	463	1.79×10^{-2}
375	1.77×10^{-4}	353	1.39×10^{-2}	467	2.04×10^{-2}
403	4.29×10^{-4}	358	1.66×10^{-2}	470	2.37×10^{-2}
405	4.96×10^{-4}	363	2.06×10^{-2}	474	2.77×10^{-2}
412	5.88×10^{-4}	368	2.58×10^{-2}	477	3.24×10^{-2}
		373	3.25×10^{-2}	480	3.76×10^{-2}
Colorado 19GPT 1000 °C Pyrolysis					
447	2.05×10^{-5}	**Estonian 1000 °C Pyrolysis**		**Chinese M-C 500 °C Pyrolysis**	
459	3.44×10^{-5}	366	6.18×10^{-4}	323	5.26×10^{-3}
478	5.41×10^{-5}	375	8.06×10^{-4}	328	5.80×10^{-3}
483	6.57×10^{-5}	375	8.54×10^{-4}	328	6.24×10^{-3}
498	9.49×10^{-5}	375	9.12×10^{-4}	332	7.40×10^{-3}
515	1.65×10^{-4}	376	9.25×10^{-4}	333	7.68×10^{-3}
518	2.19×10^{-4}	381	1.10×10^{-3}	337	9.36×10^{-3}
520	2.23×10^{-4}	398	2.33×10^{-3}	338	9.31×10^{-3}
		400	2.64×10^{-3}	342	1.10×10^{-2}
Colorado 50GPT 500 °C Pyrolysis		403	2.66×10^{-3}	343	1.13×10^{-2}
321	1.43×10^{-4}			347	1.33×10^{-2}
336	2.77×10^{-4}	**Chinese MA 500 °C Pyrolysis**		348	1.32×10^{-2}
340	2.66×10^{-4}	292	2.56×10^{-3}	352	1.62×10^{-2}
350	4.28×10^{-4}	297	3.06×10^{-3}	353	1.60×10^{-2}
363	5.61×10^{-4}	302	4.12×10^{-3}	357	1.81×10^{-2}
365	6.77×10^{-4}	307	5.11×10^{-3}	358	1.82×10^{-2}
370	7.29×10^{-4}	308	5.46×10^{-3}		
372	8.66×10^{-4}	312	6.33×10^{-3}	**Chinese M-C 1000 °C Pyrolysis**	
		313	6.69×10^{-3}	439	8.09×10^{-5}
Colorado 50GPT 1000 °C Pyrolysis		317	8.22×10^{-3}	447	1.09×10^{-4}
440	4.47×10^{-4}	322	9.84×10^{-3}	459	1.79×10^{-4}
464	1.18×10^{-3}	323	1.06×10^{-2}	462	2.05×10^{-4}
465	1.19×10^{-3}	327	1.20×10^{-2}	478	2.77×10^{-4}
473	1.73×10^{-3}	328	1.27×10^{-2}	488	4.72×10^{-4}
480	2.05×10^{-3}	332	1.50×10^{-2}	498	5.37×10^{-4}
482	2.26×10^{-3}	333	1.59×10^{-2}	501	5.95×10^{-4}
488	2.87×10^{-3}	337	1.86×10^{-2}	503	6.75×10^{-4}
503	5.01×10^{-3}	338	1.98×10^{-2}	513	9.32×10^{-4}
		343	2.37×10^{-2}	517	9.86×10^{-4}
		348	2.88×10^{-2}	523	1.11×10^{-3}
		353	3.42×10^{-2}	536	1.69×10^{-3}
		358	3.79×10^{-2}		

surface retorting) to explore the semicoke characteristics following decomposition of the oil shale mineral carbonate, which occurs at approximately the upper bound of surface retorting. Some types of in situ retorting involve a combustion step as a heat source at temperatures in excess of the carbonate decomposition temperature, such that some of the residual organic carbon is actually gasified by the evolving CO_2.[30] Therefore, the two selected pyrolysis temperatures provide semicokes that are, in one case, representative of fresh surface retorting byproducts and, in the other case, representative of conditions that may be obtained during in situ retorting or any semicoke combustion process. These choices enable a comparison of semicokes before and after carbonate decomposition while avoiding the complicating effects of CO_2 gasification in the kinetics reported. Fischer Assay oil yields, in units of gallons of oil per ton of oil shale (GPT), were calculated from the kerogen content of the shales, according to Cook et al.[18] Calculated GPT values from our laboratory aligned well with those from the shale providers (reported in Table 1). In a previous paper, we have described the techniques used and data obtained in the determination of the organic char portion, as well as the resulting porosities of each of these samples.[16]

The oxidation of any organic char is comprised of a complex series of chemical reactions; as such, it is often represented by an overall or global kinetic analysis.[19] The overall oxidation conversion rate (r) of semicarbonaceous systems such as coal char and wood char is expressed as a variety of functions. Some expressions include a surface area or pore geometry factor term; others, such as the one we consider herein, include a rate of oxidation of residual organic carbon as a function of oxygen partial pressure:

$$r = \frac{dx}{dt} = k(1 - x)P^n \quad (1)$$

where k is a rate constant, P the partial pressure of oxygen present, n the oxygen-dependent reaction order, and x the fractional extent of conversion at any time t. The latter can be obtained from experimental data as follows:

dx.doi.org/10.1021/ef3015052 | Energy Fuels 2013, 27, 666−672

Table 2. Critical Temperature, Activation Energy, Pre-exponential Factor, and Reaction Order for Semicokes Pyrolyzed at 500 and 1000 °C with Previously Determined Fischer Assay GPT, Organic Char Content, and BET Specific Surface Area[a]

sample	Fischer assay (GPT)	organic char (wt %)	critical temperature (°C)	activation energy (kJ/mol)	pre-exponential factor (s^{-1})	reaction order	BET area (m^2 g^{-1} char)
Colorado 19 GPT, 500 °C pyrolysis	21	2.6	380	108.3 ± 4.6	$1.0 \times 10^5 \pm 1.3 \times 10^4$	N/D	301
Colorado 19 GPT, 1000 °C pyrolysis	21	1.7	464	150.4 ± 6.4	$1.7 \times 10^6 \pm 3.0 \times 10^5$	N/D	136
Colorado 50 GPT, 500 °C pyrolysis	51	6.2	371	106.9 ± 5.0	$3.7 \times 10^5 \pm 6.2 \times 10^4$	0.65	338
Colorado 50 GPT, 1000 °C pyrolysis	51	2.1	464	175.0 ± 3.0	$2.9 \times 10^9 \pm 1.7 \times 10^8$	N/D	362
Estonian, 500 °C pyrolysis	77	9.1	378	130.3 ± 5.0	$1.1 \times 10^9 \pm 1.7 \times 10^8$	0.60	332
Estonian, 1000 °C pyrolysis	77	7.9	493	151.2 ± 4.9	$1.3 \times 10^9 \pm 2.9 \times 10^7$	0.68	468
Chinese M-A, 500 °C pyrolysis	45	17.3	347	127.3 ± 1.0	$1.5 \times 10^9 \pm 3.2 \times 10^8$	0.61	306
Chinese M-A, 1000 °C pyrolysis	45	11.4	494	195.4 ± 7.2	$1.3 \times 10^{12} \pm 1.4 \times 10^{10}$	0.72	341
Chinese M-C, 500 °C pyrolysis	38	8.0	367	115.8 ± 2.3	$7.2 \times 10^7 \pm 3.6 \times 10^7$	0.55	370
Chinese M-C, 1000 °C pyrolysis	38	4.7	500	146.9 ± 3.2	$5.1 \times 10^6 \pm 2.5 \times 10^5$	N/D	552

[a]Data taken from ref 16.

$$x = \frac{m_i - m_t}{m_i - m_c} \quad (2)$$

where m_i is the initial mass of the semicoke (after drying), m_t the mass at time t, and m_c the mass of the semicoke following complete loss of the organic char portion of the semicoke.

Integrating eq 1 gives

$$\ln(1 - x) = -kP^n(t - t_0) \quad (3)$$

The rate constant (k) can be obtained from the Arrhenius expression under the assumption that the apparent oxidation of char is an overall first-order reaction:

$$k = A \exp\left(-\frac{E_a}{RT}\right) \quad (4)$$

where A is the frequency factor, also known as pre-exponential factor, E_a the activation energy, R the universal gas constant, and T the absolute temperature.[20−22] The overall activation energy of the oxidation reaction can be obtained by plotting the logarithmic conversion rate versus the inverse absolute temperature, $1/T$. The slope of the curve equals $-E_a/R$. The pre-exponential factor determined from the Arrhenius equation assumes an independence from temperature; it is an empirical relationship.

The kinetic parameters of each oil shale semicoke were determined using both a TA Instruments Model 951 thermogravimetric analyzer (TGA) and a Mettler Toledo DSC/TGA-1, following the same overall procedure. Between 5 and 10 mg of semicoke were added to a platinum pan (TA Instruments), or 3−5 mg of semicoke were added to an alumina crucible (Mettler Toledo) in each TGA to achieve a thin layer of semicoke covering the bottom of the pans. All samples were heated to 120 °C and held at this temperature for 20 min to ensure moisture removal; experiments did not proceed until a constant mass was obtained at this temperature.

Isothermal measurement of the oxidation rates of semicokes occurred in dry air flowing at ∼175 cm^3 min^{-1}. Each sample was subjected to at least six different temperature plateaus and at each the rate of oil shale semicoke oxidation mass loss was measured. Another measure of reactivity of char, the "critical temperature," was also determined. The critical temperature, as defined by Charpenay et al.,[23] is the temperature at which the carbon mass loss rate is equal to 0.065 min^{-1}. It is a gauge of char reactivity; the lower the critical temperature, the higher the reactivity of the sample. For char oxidation, this rate is easily measurable, but still low enough to ensure operation within the kinetically controlled oxidation regime without influence of mass transfer limitations. We chose to compare our oil shale semicokes on this basis to coal chars for which this reactivity measure has been previously published.

Using the TGA, isothermal mass loss rates were measured as a function of varying partial pressures of oxygen (in a mixture with nitrogen, at 1 atm. total pressure) and analyzed for the oxidation reaction order. Each sample, following moisture removal as described above, was held at its respective temperature for 40 min while a series of four gases with varying mole fractions of O_2:N_2 (100:0, 25:75, 50:50, 21:79) (supplied by Corp. Bros., USA) flowed through the TGA at flow rates between 170 and 180 cm^3 min^{-1}, as controlled by an Omega III mass flowmeter. Each semicoke was run a minimum of two times in each gas mixture to ensure reproducibility. The apparent oxidation rate of the residual carbon remaining in the semicoke, as a function of unknown reaction order (n) and oxygen partial pressure (P), can be obtained from eq 1 by plotting ln r vs ln P, which provides the reaction order with respect to the partial pressure of oxygen. The slopes of the straight lines are the apparent reaction orders n. The measurements taken under varying partial pressures of oxygen used to determine the reaction order of each shale semicoke were all performed on TA Instruments TGA equipment. In this instance, all the 500 °C pyrolyzed samples were tested at 380 °C and the 1000 °C samples were tested at 480 °C, within ±15 °C of the critical temperature of all of the samples pyrolyzed at their respective temperature.

RESULTS AND DISCUSSION

Table 1 details the raw data used to determine E_a and A using the Arrhenius equation. Results from the isothermal determination of the activation energy and pre-exponential factor and determination of the overall oxidation rate constants are given in Table 2. The pyrolysis temperature clearly impacts the oxidation kinetics of the oil shale semicokes. As seen in Table 2,

dx.doi.org/10.1021/ef3015052 | Energy Fuels 2013, 27, 666−672

our critical temperatures range from 347 °C to 380 °C for semicokes pyrolyzed at 500 °C, and from 464 °C to 500 °C for semicokes pyrolyzed at 1000 °C, indicating a higher reactivity for the 500 °C pyrolyzed samples. For comparison, critical temperatures determined for chars produced from pyrolysis of Argonne premium coals range from 430 °C to 519 °C.[23] These oil shale semicokes are thus of comparable reactivity to the Charpenay et al. chars. The critical temperature values also provided a relevant temperature range for performing our kinetic experiments to obtain measurable rates that are low enough to not be subject to mass-transfer limitations.

Figure 1 shows the significant influence of pyrolysis temperature on measured oxidation rates, consistent with the

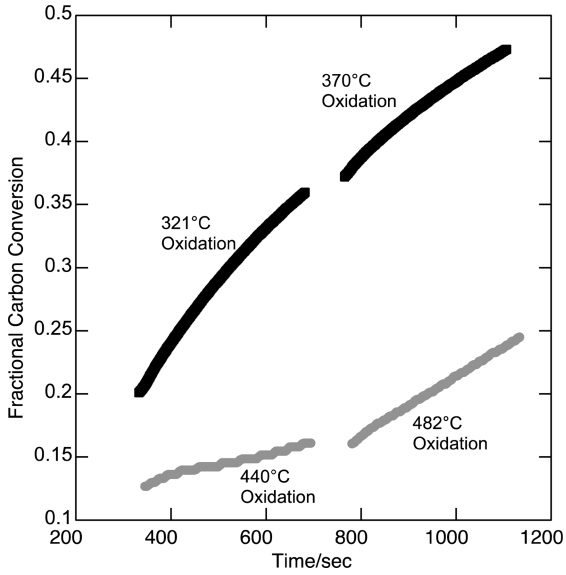

Figure 1. Fractional carbon conversion versus time for Colorado 50GPT semicokes; 500 °C pyrolyzed semicokes measured at 321 and 370 °C (black); 1000 °C semicokes measured at 440 and 482 °C (gray).

process of thermal annealing.[30] Results are shown for the Colorado 50 GPT semicoke pyrolyzed at 500 and 1000 °C. Fractional carbon conversion, as a function of time, is shown at two oxidation temperatures of each semicoke, at char conversions of <50%. The oxidation rate of the 500 °C semicoke at 321 °C is significantly greater than that of the 1000 °C semicoke oxidized at 440 °C. This general result holds across all shale samples, regardless of their geographic origin, showing that the process of thermal annealing applies to these chars, just as it does to most other types of carbons.[30] Figure 2 shows conversion for the Estonian 500 °C semicoke at 360, 375, 381, and 400 °C, used to determine the rate constant, k. We find activation energies for the 500 °C pyrolyzed semicokes in the range of 107−130 kJ mol^{-1}, with the two 500 °C Colorado semicokes having the lowest activation energies (see Table 2). For the shales pyrolyzed at 1000 °C, the Colorado 19 GPT gives an activation energy of 150 kJ mol^{-1}, while the Colorado 50 GPT 1000 °C semicoke gives a value of E_a = 175 kJ mol^{-1}; the Chinese C sample showed the lowest activation energy among the 1000 °C pyrolyzed semicokes (147 kJ mol^{-1}).

The kinetic parameters are clearly a function of pyrolysis temperature, as already noted. While the values for different oil shales differ, they all show a consistent trend of an increase of

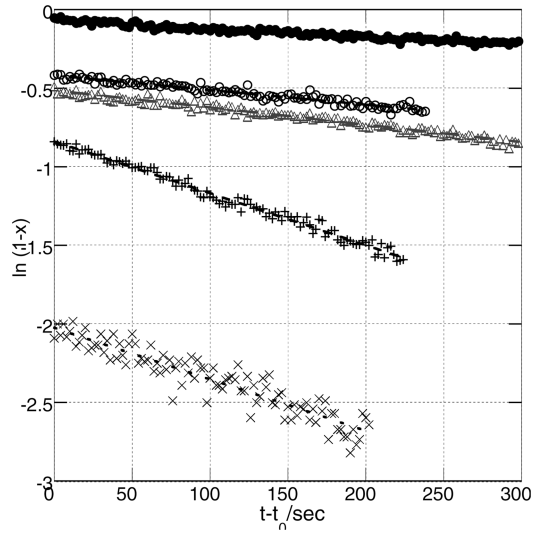

Figure 2. Fractional conversion as a function of time for Estonian semicokes pyrolyzed at 500 °C taken at varying temperatures: (●) 360 °C, (○) 375 °C, (△) 380 °C, (+) 400 °C, and (×) 418 °C.

activation energy with heat-treatment temperature. In addition, while the shale's origin dictates the characteristics of its raw kerogen, the similarity of all the T_{crit} values shows that the semicokes are fundamentally quite similar. It should also be noted that the shale's origin determines its mineral composition.[25] Hutton classified oil shales according to formation environment: terrestrial, lacustrine, and marine. These classifications were further subdivided according to organic origin and age.[26] These characteristics of the oil shale will, logically, influence the properties of the oil shale semicokes that are produced. This is clearly evidenced in the organic char contents remaining after pyrolysis under comparable conditions: ranging from 2.6% carbon for Colorado 19 GPT semicoke pyrolyzed at 500 °C to 17.3% present in the Chinese M-C sample pyrolyzed at the same temperature. Datangel and Goldfarb demonstrated that the heavy-metal content of oil shale and its semicokes is also dependent on both shale origin and pyrolysis temperature.[27] The residual mineral contents of the shale can play a role in influencing oxidation reactivity, because of the catalytic effect of the minerals (which were not studied here.) Thus, it is not surprising that different shales yield different rate constants.

Figure 3 shows the Arrhenius plot for the Estonian and Colorado 50 GPT semicokes pyrolyzed at 500 and 1000 °C. The linearity of the data confirm first-order kinetics, with respect to residual carbon mass, as observed by many other groups for the oxidation of oil shale semicokes.[21,22] An upward concave curve would be indicative of a reaction order of >1, or multiple simultaneous decomposition reactions, and a concave downward trend would indicates a reaction order of <1, or a set of decomposition reactions in series. Given the relatively linear Arrhenius plot over the measured temperature range—with R^2 values all greater than 0.98—the overall or global reaction order, with respect to char, is ∼1.

The reaction orders, with respect to oxygen partial pressures, reported in Table 2, are recorded at conversion levels between 20% and 40%. Figure 4 shows an example of the results, with respect to the partial pressure of oxygen for the Chinese M-A 500 °C pyrolyzed semicoke. The reaction orders, with respect to oxygen, for all the semicokes investigated herein range from

dx.doi.org/10.1021/ef3015052 | Energy Fuels 2013, 27, 666−672

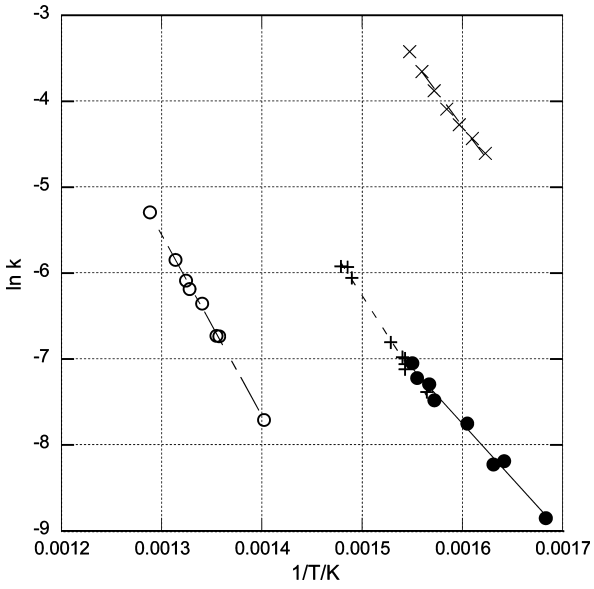

Figure 3. Arrhenius plot for Colorado 50 GPT semicokes pyrolyzed at (●) 500 °C and (○) 1000 °C and Estonian semicokes pyrolyzed at (×) 500 °C and (+) 1000 °C.

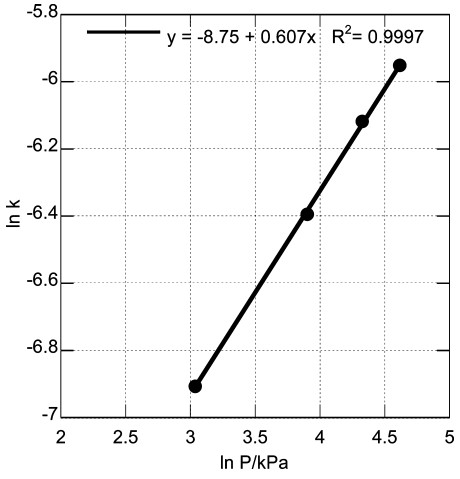

Figure 4. Determination of oxidative reaction order as a function of oxygen partial pressure for Chinese M-A oil shale semicoke pyrolyzed at 500 °C.

0.55 to 0.72, depending on the pyrolysis temperature. The oil shale semicokes pyrolyzed at 500 °C were investigated at an oxidation temperature of 380 °C, while the samples pyrolyzed at 1000 °C (less-reactive samples) were oxidized at 480 °C. The apparent reaction orders of the oil shale semicokes increase with pyrolysis temperature, and are quite similar to those for coal char and wood chars.[24,28] The 500 °C samples have reaction orders of ∼0.6, and the 1000 °C samples have reaction orders of ∼0.7. In fact, all of the orders are quite similar to those reported for an enormous range of carbons.[31] There were several oil shale semicoke samples (both Colorado 19GPT semicokes; Colorado 50GPT 1000 °C; Chinese M-C 1000 °C) for which we were not able to accurately determine the reaction order, because of the low (<5 wt %) organic char content and potential secondary reactions in the mineral portions of the char. However, we see from the data on the other semicokes that the reaction orders, with respect to oxygen, appear to be independent of shale origin.

Our data, and those of others, suggest that the final pyrolysis temperature is critical to the oxidation kinetics of the semicoke, and others have reported an effect of heating rate as well, as seen in Table 3. Qing et al. measure activation energies for oxidation in air of semicoke produced at three temperatures from oil shale from the Huadian mine in the Jilin province of China. Their samples were pyrolyzed at 2 °C min^{-1}, which is a slower rate than used here. They separated their activation energies into a low-temperature stage (up to 400 °C) and a high-temperature stage (410−650 °C). The low-temperature stage results in activation energies of 118.5, 133.9, and 233.9 kJ mol^{-1} for the Huadian semicoke pyrolyzed at 500, 600, and 700 °C, respectively. For the high-temperature stage, the activation energies for these semicoke samples were 131.7, 146.3, and 360.1 kJ mol^{-1}, respectively.[3] Hence, the same trend of increasing activation energy with increasing pyrolysis temperature was obtained, although the increase was much more significant. Fujimoto et al. found an oxidation activation energy of 81.2 kJ mol^{-1} for semicoke from Green River Colorado 24 GPT shale that was rapidly pyrolyzed at 530 °C. They found the oxidation of this rapidly pyrolyzed shale to be well-represented by a second-order reaction, with a possibility of two simultaneous first-order reactions. Fujimoto et al. concluded that char from rapid heating is 2−3 times more reactive than char from slow pyrolysis.[20] Since their reaction order, with respect to char, is quite different from that found in this study, it is unclear whether their activation energies can be directly compared to those reported here. As seen in Table 3, Han et al. also measured the oxidation activation energies of Chinese Huadian oil shale slowly pyrolyzed to 500 °C over two nonisothermal temperature ranges; the oxidation of the Huadian shale semicokes pyrolyzed at temperatures below 530 °C gave oxidation activation energies of 59.91, 67.98, and 81.05 kJ mol^{-1} for heating rates of 20, 40, and 60 °C min^{-1}, respectively. When oxidized at temperatures between 730 °C and 850 °C, the reported activation energies of the Huadian semicoke were 108.69, 81.68, and 80.45 kJ mol^{-1} at the same respective heating rates.[4] Thus, there was no clear trend of activation energy with heating rate (in one case, it increased; in the other, it decreased); however, the activation energies obtained were similar to those obtained by Fujimoto et al. However, these values of the oxidation activation energies were lower than that normally obtained for disordered carbons. The activation energies reported by Kaljuvee et al.[29] bracket the low values of Fujimoto et al. and Han et al. and the higher values obtained here. An activation energy value for Estonian oil shale char is given in the work of Ots[17] as 100 kJ/mol. This is comparable to some values reported by Kaljuvee et al. but lower that the value obtained here for the Estonian Oil shale semicoke sample pyrolyzed at 500 °C. It is not known how the heating rate in the present study compares to that used by Ots.

Our pyrolysis experiments were performed at a relatively slow heating rate (20 °C min^{-1}), which is orders of magnitude lower than what fine particles can experience in an industrial boiler, which can occur at rates of over 1000 °C s^{-1}. The published data by Qing et al. show highest activation energies for semicokes pyrolyzed at 2 °C min^{-1} to 700 °C and these values are much higher than those measured herein for semicokes pyrolyzed at 20 °C min^{-1} to temperatures of either 500 or 1000 °C.[3] It is unclear whether the difference between these studies is really due to a heating rate effect, because, again, the highest activation energies obtained by Qing et al. are not characteristic of most char oxidation processes.

dx.doi.org/10.1021/ef3015052 | Energy Fuels 2013, 27, 666−672

Table 3. Activation Energies as Functions of Final Pyrolysis Temperature and Heating Rate, Oxidation Temperature Range, and Shale Origin across the Literature Compared to This Work

final pyrolysis temperature (°C)	pyrolysis heating rate (°C min^{-1})	oxidation method	oxidation temperature range (°C)	activation energy (kJ mol^{-1})	kinetics model	ref
Colorado 24GPT						
530	rapid	isothermal	384−474	81.2	Arrhenius equation	20
Estonian (Isoconversional Oxidation)						
not specified	rapid	isoconversional	200−485	67.3−100.9	model-free kinetics (Friedman)	29
not specified	rapid	isoconversional	330−700	81.3−86.1	model-free kinetics (Friedman)	29
not specified	rapid	isoconversional	465−870	182.7−185.8	model-free kinetics (Friedman)	29
Colorado 19GPT						
500	20	isothermal	352−412	108.3	Arrhenius equation	this work
1000	20	isothermal	447−520	150.4	Arrhenius equation	this work
Colorado 50GPT						
500	20	isothermal	321−372	106.9	Arrhenius equation	this work
1000	20	isothermal	440−503	175.0	Arrhenius equation	this work
Estonian (Isothermal Oxidation)						
500	20	isothermal	343−373	130.3	Arrhenius equation	this work
1000	20	isothermal	366−403	151.2	Arrhenius equation	this work
Chinese M-A						
500	20	isothermal	292−358	127.3	Arrhenius equation	this work
1000	20	isothermal	460−480	195.4	Arrhenius equation	this work
Chinese M-C						
500	20	isothermal	323−358	115.8	Arrhenius equation	this work
1000	20	isothermal	439−536	146.9	Arrhenius equation	this work
Chinese Huadian (Isothermal Oxidation)						
500	2	isothermal	<400	118.5	Coats and Redfern	3
500	2	isothermal	410−650	131.7	Coats and Redfern	3
600	2	isothermal	<400	133.9	Coats and Redfern	3
600	2	isothermal	410−650	146.3	Coats and Redfern	3
700	2	isothermal	<400	233.9	Coats and Redfern	3
700	2	isothermal	410−650	360.1	Coats and Redfern	3
Chinese Huadian (Various Oxidation Rates)						
500	1.5−3.5	20 °C/min	<530	59.91	Arrhenius equation	4
500	1.5−3.5	20 °C/min	730−850	108.69	Arrhenius equation	4
500	1.5−3.5	40 °C/min	<530	67.98	Arrhenius equation	4
500	1.5−3.5	40 °C/min	730−850	81.68	Arrhenius equation	4
500	1.5−3.5	60 °C/mm	<530	81.05	Arrhenius equation	4
500	1.5−3.5	60 °C/mm	730−850	80.45	Arrhenius equation	4

The relatively low overall activation energies obtained here for the oil shale semicokes pyrolyzed at 500 °C are associated with their low degree of carbonization.[9,15] Shales pyrolyzed at lower temperatures will tend to have a higher volatile content, a higher degree of disorder, and higher hydrogen and oxygen contents than those pyrolyzed at higher temperatures;[16,17,20] at high pyrolysis temperatures, the combustible matter remaining is mostly elemental carbon.[4] Ots shows that the C/H mass ratio in char can be in the range of 25−30, which makes oil shale semicokes more reactive toward oxygen than if they were truly composed of pure carbon. The same study also shows that the combustion rate of oil shale char in the kinetically controlled region decreases with an increase in C/H ratio, which supports the findings of the present study[17] and is consistent with the concept of annealing.[30]

The high oxidation reactivities of oil shale semicokes, especially those pyrolyzed at 500 °C, make them an attractive co-fired fuel for the generation of energy or syngas production. As a co-fired fuel with raw oil shale, Wang et al. note that the rapid combustion of organic material in oil shale improves the co-combustion characteristics of various semicoke−oil shale blends. However, they note that as the semicoke fraction increases, the activation energy increases presumably because the raw oil shale is characterized by a lower activation energy than the heat-treated semicoke, consistent with the results of this study.[12] In agreement with these studies, our data show

dx.doi.org/10.1021/ef3015052 | Energy Fuels 2013, 27, 666−672

that, as pyrolysis temperature increases, the ability to co-fire large quantities of semicoke may decrease because of higher activation energies and lower organic char fractions.

CONCLUSIONS

Overcoming obstacles to the commercial retorting of oil shale to produce oil requires one to address the environmental impact of the semicoke waste. One way of utilizing this waste is to co-combust the semicoke with parent fuel or other fuel sources. However, our data and others in the literature show that it is imperative to know the conditions under which the shale was retorted. Examination of the literature on oil shale semicoke oxidation kinetics still offers a somewhat confusing picture, with different workers recently reporting very different kinetic constants. It is unclear what the origin of these differences might be, although it seems unlikely to be attributable to be heating rate effects.

In general, the activation energy required to oxidize oil shale semicokes clearly increases as the retort temperature increases: this is likely due to the progressive increase in C/H ratio in oil shale semicoke. Similarly, semicokes pyrolyzed at higher temperatures also exhibit slower char oxidation rates. The oxidation reactions of oil shale semicokes produced at 500 and 1000 °C at a heating ramp rate of 20 °C min^{-1} appear well-represented by the Arrhenius equation, with an overall reaction order of 1, with respect to remaining carbon. The reaction orders, with respect to the partial pressures of oxygen, ranged from 0.55 to 0.72, with the semicokes pyrolyzed at higher temperatures exhibiting slightly higher orders. Again, this is entirely consistent with the low-temperature oxidation kinetics reported for a large number of different types of chars.

AUTHOR INFORMATION

Corresponding Author

*Tel.: 603 862 1917. E-mail: JillianLGoldfarb@gmail.com.

Notes

The authors declare no competing financial interest.

ACKNOWLEDGMENTS

The authors acknowledge the support of the University of New Hampshire Hamel Center for Undergraduate Research INCO590 Student Research Experience funded through the College of Engineering and Physical Sciences. The authors thank Dr. Jianrong Qiu (Huazhong University of Science and Technology, China) for providing the Chinese oil shale samples and Rein Rootam and Tõnu Pihu (Tallinn University of Technology, Estonia) for providing the Estonian oil shale sample.

REFERENCES

(1) Chopra, S.: Lines, L. R.; Schmitt, D. R.; Batzle, M. Heavy-oil Reservoirs: Their Characterization and Production. In: *Heavy Oils: Reservoir Characterization and Production Monitoring*, Geophysical Developments Series No. 13. Chopra, S.; Lines, L.R.; Schmitt, D.R.; Batzle, M.L., Eds.; Society of Exploration Geophysicists: Tulsa, OK, USA, 2010; pp 1−65.

(2) Kahru, A.; Põllumaa, L. *Oil Shale* **2006**, *23*, 23−53.

(3) Qing, W.; Baizhong, S.; Xiahua, W.; Jingru, B.; Jian, S. *Oil Shale* **2006**, *23*, 328−339.

(4) Han, X. X.; Jiang, X. M.; Cui, Z. G. *J. Therm. Anal. Calorim.* **2008**, *92*, 595−600.

(5) Trikkel, A.; Kuusik, R.; Martins, A.; Pihu, T.; Stencel, J. M. *Fuel Process. Technol.* **2008**, *89*, 756−763.

(6) Datangel, B.; Goldfarb, J. L. *Energy Fuels* **2011**, *25*, 3522−3529.

(7) *2007 Survey of Energy Resources*; World Energy Council (WEC): London, U.K., 2007. (http://www.worldenergy.org/documents/ser2007_final_online_version_1.pdf; accessed September 4, 2012).

(8) Mõtlep, R.; Kirsimäe, K.; Talviste, P.; Puura, E.; Jürgenson, J. *Oil Shale* **2007**, *24*, 405−422.

(9) Kikas, V. *Oil Shale* **1988**, *5*, 15−28.

(10) Kikas, V.; Piksarv, E.; Dokelin, S.; Hain, A. *Cement* **1983**, *11*, 16−17.

(11) Pihu, T.; Arro, H.; Prikk, A.; Rootamm, R.; Konist, A.; Kirsimäe, K.; Liira, M.; Mõtlep, R. *Fuel* **2012**, *93*, 172−180.

(12) Wang, W.; Wang, H.; Sun, B.; Bai, J.; Guan, X. *Fuel* **2009**, *88*, 1520−1529.

(13) Jaber, J. O.; Probert, S. D. *Appl. Energy* **1997**, *58*, 161−175.

(14) Yan, J.; Jiang, X.; Han, X. *Energy Fuels* **2009**, *23*, 5792−5797.

(15) Siirde, A.; Roos, I.; Martins, A. *Oil Shale* **2011**, *28*, 1−4.

(16) Külaots, I.; Goldfarb, J. L.; Suuberg, E. M. *Fuel* **2010**, *89*, 3300−3306.

(17) Ots, A. Oil Shale Fuel Combustion. In: *Eesti Energia*. Ots, A.; Tyson, T.; McQuillen, M., Eds.; Tallinn, Estonia; 2004: pp 13−17, 49−58.

(18) Cook, E. W. *Fuel* **1974**, *53*, 146−151.

(19) Burnham, A. K.; Braun, R. L. *Energy Fuels* **1999**, *13*, 1−22.

(20) Fujimoto, F. D.; Braun, R. L.; Taylor, R. W.; Morris, C. J. *Energy Fuels* **1987**, *1*, 320−323.

(21) Thompson, W. J.; Soni, Y. *In Situ* **1980**, *4*, 61−77.

(22) Sohn, H. Y.; Kim, S. K. *Ind. Eng. Chem. Process Des. Dev.* **1980**, *19*, 550−555.

(23) Charpenay, S.; Serio, M. A.; Solomon, P. R. In *Twenty-Fourth Symposium (International) on Combustion*; The Combustion Institute: Pittsburgh, PA, 1992; p 1189.

(24) Kaijtani, S.; Suzuki, N.; Ashizawa, A.; Hara, S. *Fuel* **2006**, *85*, 163−169.

(25) Dyni, J. R. *Geology and Resources of Some World Oil-Shale Deposits*. Scientific Investigations Report 2005-5294, 2005. (Available via the Internet at http://pubs.usgs.gov/sir/2005/5294/pdf/sir5294_508.pdf, accessed November 30, 2012.)

(26) Hutton, A. C. *Int. J. Coal Geol.* **1987**, *8*, 203−231.

(27) Datangel, B.; Goldfarb, J. L. *Energy Fuels* **2011**, *25*, 3522−3529.

(28) Janse, A.; de Jonge, H. G.; Prins, W.; van Swaaij, W. P. M. *Ind. Eng. Chem. Res.* **1998**, *37*, 3909−3918.

(29) Kaljuvee, T.; Keelmann, M.; Trikkel, A.; Kuusik, R. *J. Thermal. Anal. Calorim.* **2011**, *105*, 395−403.

(30) Manor, Y.; Suuberg, E. M.; Ho, M.; Toor, H. L. In *Nineteenth Symposium on Combustion*; The Combustion Institute: Pittsburgh, PA, 1982; pp 1093−1103.

(31) Suuberg, E. M.; Wojtowicz, M.; Calo, J. M. In *Twenty-Second (International) Symposium on Combustion*; The Combustion Institute: Pittsburgh, PA, 1988; pp 79−87.